5-2017

IMF Dependence of Energetic Oxygen and Hydrogen Ion Distributions in the Near-Earth Magnetosphere

H. Luo
Chinese Academy of Sciences

E. A. Kronberg
Max Planck Institute for Solar System Research

K. Nykyri
Embry-Riddle Aeronautical University, nykyrik@erau.edu

K. J. Trattner
University of Colorado, Boulder

P. W. Daly
Max Planck Institute for Solar System Research

See next page for additional authors

Scholarly Commons Citation

Luo, H., E. A. Kronberg, K. Nykyri, K. J. Trattner, P. W. Daly, G. X. Chen, A. M. Du, and Y. S. Ge (2017), IMF dependence of energetic oxygen and hydrogen ion distributions in the near-Earth magnetosphere, J. Geophys. Res. Space Physics, 122, 5168–5180, doi:10.1002/2016JA023471

AGU PUBLICATIONS

JGR

Journal of Geophysical Research: Space Physics

RESEARCH ARTICLE
10.1002/2016JA023471

Key Points:
- We present the statistical observation of energetic ion distributions in the dayside magnetosphere and near-Earth plasma sheet
- The dawn-dusk asymmetry of the distribution shows strong IMF dependence
- The location of magnetic reconnection at the magnetopause influences the dawn-dusk asymmetry

Supporting Information:
- Supporting Information S1

Correspondence to:
H. Luo,
luohao06@gmail.com

Citation:
Luo, H., E. A. Kronberg, K. Nykyri, K. J. Trattner, P. W. Daly, G. X. Chen, A. M. Du, and Y. S. Ge (2017), IMF dependence of energetic oxygen and hydrogen ion distributions in the near-Earth magnetosphere, *J. Geophys. Res. Space Physics*, *122*, 5168–5180, doi:10.1002/2016JA023471.

Received 14 SEP 2016
Accepted 17 APR 2017
Accepted article online 24 APR 2017
Published online 11 MAY 2017

IMF dependence of energetic oxygen and hydrogen ion distributions in the near-Earth magnetosphere

H. Luo[1,2,3], E. A. Kronberg[2,4], K. Nykyri[5], K. J. Trattner[6], P. W. Daly[2], G. X. Chen[1,3], A. M. Du[1,3], and Y. S. Ge[1,3]

[1]Key Laboratory of Earth and Planetary Physics, Institute of Geology and Geophysics, Chinese Academy of Sciences, Beijing, China, [2]Max Planck Institute for Solar System Research, Göttingen, Germany, [3]College of Earth Sciences, University of Chinese Academy of Sciences, Beijing, China, [4]Department of Earth and Environmental Sciences, Ludwig-Maximilians University, Munich, Germany, [5]Centre for Space and Atmospheric Research and Department of Physical Sciences, Embry-Riddle Aeronautical University, Daytona Beach, Florida, USA, [6]Laboratory for Atmospheric and Space Physics, University of Colorado Boulder, Boulder, Colorado, USA

Abstract Energetic ion distributions in the near-Earth plasma sheet can provide important information for understanding the entry of ions into the magnetosphere and their transportation, acceleration, and losses in the near-Earth region. In this study, 11 years of energetic proton and oxygen observations (> ~274 keV) from Cluster/Research with Adaptive Particle Imaging Detectors were used to statistically study the energetic ion distributions in the near-Earth region. The dawn-dusk asymmetries of the distributions in three different regions (dayside magnetosphere, near-Earth nightside plasma sheet, and tail plasma sheet) are examined in Northern and Southern Hemispheres. The results show that the energetic ion distributions are influenced by the dawn-dusk interplanetary magnetic field (IMF) direction. The enhancement of ion intensity largely correlates with the location of the magnetic reconnection at the magnetopause. The results imply that substorm-related acceleration processes in the magnetotail are not the only source of energetic ions in the dayside and the near-Earth magnetosphere. Energetic ions delivered through reconnection at the magnetopause significantly affect the energetic ion population in the magnetosphere. We also believe that the influence of the dawn-dusk IMF direction should not be neglected in models of the particle population in the magnetosphere.

1. Introduction

It is well known that the energetic ions (> ~100 keV) in the near-Earth plasma sheet are important consequences of transport and acceleration in the magnetosphere. The ions cannot be accelerated by quasi-stationary dawn-dusk electric field like Speiser acceleration [*Speiser*, 1965] or betatron acceleration [e.g., *Sarafopoulos et al.*, 2001] alone to energies higher than typical tail potential drop. Substorm-associated magnetic field reconfiguration is also thought to be an important process to accelerate the ions to high energy when they are transported to the near-Earth region from the magnetotail [e.g., *Nosé et al.,* 2000a, 2000b; *Ono et al.*, 2009; *Grigorenko et al.*, 2017]. Acceleration of energetic ions higher than ~140 keV is reported in both earthward and tailward fast flows, which are associated with the near-Earth X line [*Luo et al.*, 2014]. Magnetic reconnection-associated structures such as flux ropes and plasmoids in the distant magnetotail are also thought to be the regions where the tailward energetic oxygen flux is significantly increased [*Wilken et al.*, 1995; *Zong et al.*, 1997, 1998]. *Grigorenko et al.* [2015] found that ion resonant interactions with the low-frequency electromagnetic fluctuations are important for ion acceleration inside plasmoids. The geomagnetic and solar wind-dependent spatial distributions of oxygen ions and protons at energies from 274 to 955 keV were statistically established by *Kronberg et al.* [2015] based on 7 years of Cluster observations. The discussion on dawn-dusk asymmetries of ion distributions in the plasma sheet has been reviewed by *Kronberg et al.* [2017].

Ions can enter the magnetosphere not only via acceleration processes in the magnetotail but also through reconnection at the magnetopause. Energetic neutral atom observations (0.9–1.5 keV) in the cusp show an asymmetry in fluxes explained by the magnetic reconnection at the magnetopause [*Petrinec et al.*, 2011]. Other studies showed that the energetic ions observed in the cusp have similar spectral features as those accelerated at the quasi-parallel bow shock [*Trattner et al.*, 2001]. Moreover, they showed that energetic ions from the quasi-parallel bow shock enter the diamagnetic cavity along newly reconnected field lines [*Trattner et al.*, 2011].

The diamagnetic cavity in the high-latitude cusp region is also thought to be a possible source of energetic ions in the dayside magnetosphere and near-Earth plasma sheet [e.g., *Chen and Fritz*, 1998; *Fritz et al.*, 2000; *Fritz et al.*, 2012]. The diamagnetic cavity is a region with enhanced plasma pressure and decreased magnetic field strengths formed by the magnetic reconnection in the high-latitude magnetopause [e.g., *Nykyri et al.*, 2011a, *Adamson et al.*, 2012]. This region is able to trap charged particles. *Nykyri et al.* [2011b, 2012] showed that ions and electrons can be locally accelerated up to 50 keV in the diamagnetic cavity if they are trapped for sufficiently long time and their drift paths coincide with the gradient of reconnection quasi-potential. The amount of acceleration depends on the magnetic field strength that is reconnecting and generating the quasi-potential. Higher energies are also possible if particles can be recycled via this quasi-potential, but some particles will also be lost into the magnetosheath or ionosphere.

The dependence of the ion distribution on the interplanetary magnetic field (IMF) direction hints at the nature of the physical processes at work. Previous studies were focused on the response of the ion distributions depending on the northward/southward direction of the IMF. The influence of the dawn-dusk IMF direction on the ion distribution in the near-Earth magnetosphere has been studied by, e.g., *Petrinec et al.* [2011] (cusp region, 0.9–1.5 keV) and *Liao et al.* [2010] (transport from cusp $<$40 keV/*e*) who used observations and by *Welling et al.* [2011] who used MHD simulations (ring current). But they only focused on the ions with lower energy.

It was shown that the energetic ion flux ($>$274 keV) in the near-Earth magnetosphere depends on the IMF clock angle [*Kronberg et al.*, 2012]. However, the influence of the dawn-dusk IMF direction on the distribution of energetic ions ($>$274 keV, much higher energies than those considered in the previous studies) at the dayside and the plasma sheet has still not been studied. Moreover, the source of the energetic ions in the dayside magnetosphere is still not completely understood, and our study could provide the information on the sources for the energetic ions in both the dayside magnetosphere and the nightside plasma sheet in the near-Earth region. Additionally, we separate the Northern and Southern Hemispheres, which has not been done before at these energies.

In summary in this study, we present statistical observations of the energetic ion distributions in the dayside and the near-Earth plasma sheet for both the Northern and Southern Hemispheres and their dependence on the dawn-dusk IMF. We check if the distributions can be explained by the location of the reconnection at the magnetopause that can be related to a source of energetic ions in the magnetosphere.

2. Instrumentation and Data Description

Omnidirectional flux of oxygen and protons during years 2001–2011 from the RAPID experiment (Research with Adaptive Particle Imaging Detectors) on board Cluster 4 is used in this study. The detailed information about the Cluster mission and RAPID experiment is given by *Escoubet et al.* [1997] and *Wilken et al.* [2001], respectively. The energy channels for H^+ and O^+ are not the same. In order to compare the observations between H^+ and O^+, we need to put their energy channels into the same range. The detailed methodology for adjusting the energy channels can be found in Appendix A in *Kronberg et al.* [2012]. In this study, 3 min averages of integrated intensity of H^+ with energy from ~274 keV to ~962 keV and O^+ from ~274 keV to ~948 keV are used to investigate the energetic ion distribution in the dayside magnetosphere and the nightside plasma sheet. The slight difference in upper energy (962 keV and 948 keV) does not affect our results. The plasma beta calculated based on Cluster Ion Spectrometry (CIS)/CODIF plasma pressure [*Rème et al.*, 2001] and the magnetic field measurements from the fluxgate magnetometer [*Balogh et al.*, 2001] are set to be larger than 0.2 and less than 10 to confine the observations in the plasma sheet [*Baumjohann et al.*, 1990; *Grigorenko et al.*, 2012]. There are several operational modes for the instruments on board Cluster spacecraft. For example, for the CIS instrument, there are the solar wind modes, the magnetospheric modes, the magnetosheath modes, the retarding potential analyzer mode, and a calibration and test mode. These modes correspond to different energy sweeping schemes and different combinations of telemetry products transmitted. In our study, we are only interested in the energetic ions in the magnetosphere. We select data with magnetospheric mode 13 to confine the observations in the magnetosphere and avoid errors introduced by nonoptimal modes [*Rème et al.*, 2001; *Dandouras et al.*, 2006]. Solar wind data are from OMNI database.

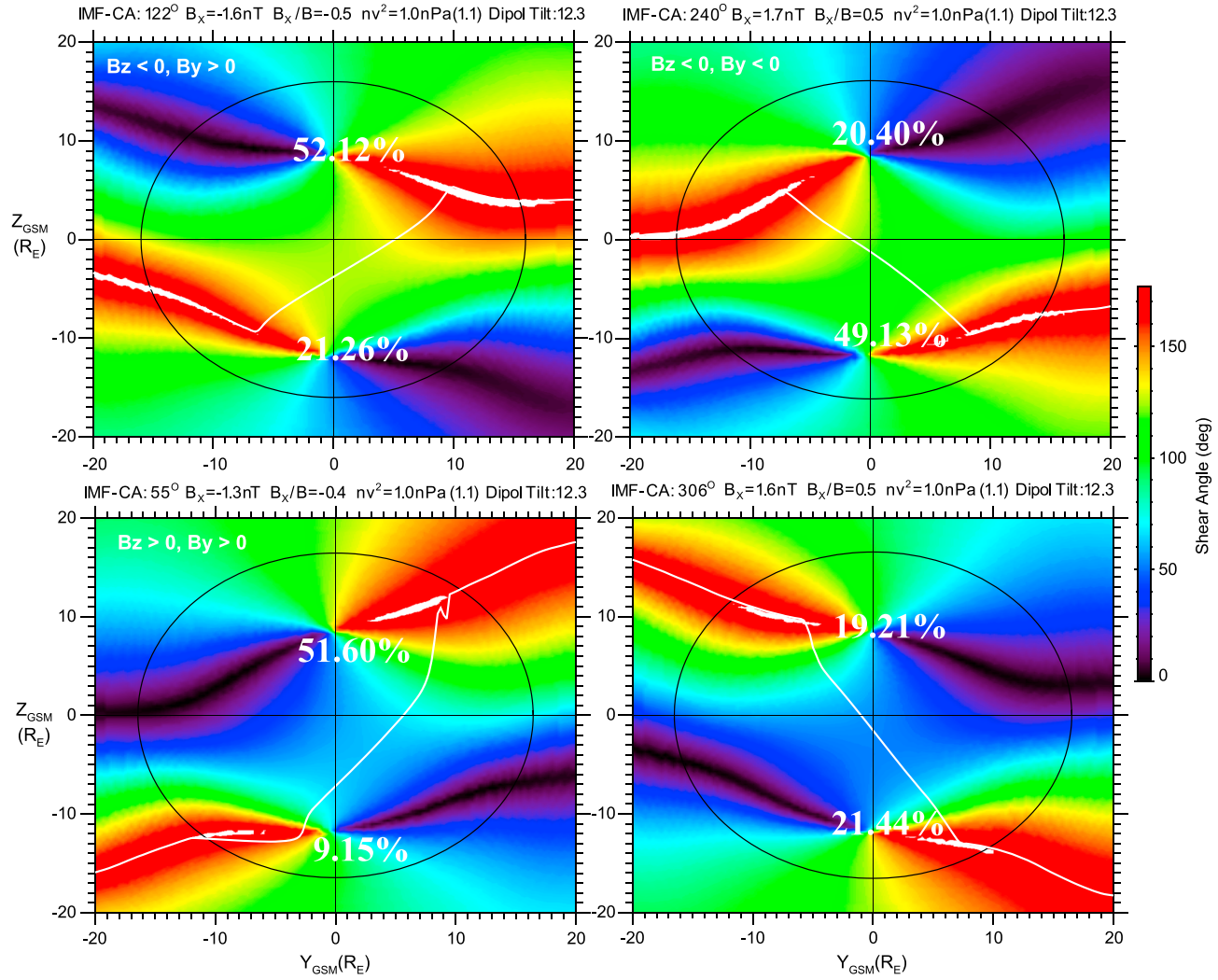

Figure 1. The magnetopause shear angle under IMF $B_z < 0, B_y > 0$, $B_z < 0, B_y < 0$, $B_z > 0, B_y > 0$, $B_z > 0, B_y < 0$ as seen from the Sun. The shear angles were determined by the magnetic field direction of the T96 model and median values (list in Table 3) of the solar wind conditions where our observations are made in Figures 2–5. Red areas represent magnetopause regions where the geomagnetic field and the IMF are antiparallel within 150° to 180°. White regions embedded in the red regions represent the line of maximum magnetic shear angles which are thought to be the most likely location for reconnection to occur. The black circle in each panel represents the location of the $x = 0$ plane, which separates the dayside magnetopause (inside the circle) from the nightside magnetopause (outside the circle) of the Earth. The values plotted over each panel are asymmetry indexes for protons in $0\ R_E < Z < 4\ R_E$ under southward IMFs and $4\ R_E < Z < 8\ R_E$ under northward IMFs.

In order to confine the observations to the plasma sheet, we need to exclude the cusp region as it usually has the same plasma beta value range as in the plasma sheet. Data with $|Z\ (\mathrm{GSM})| < 8\ R_E$ are selected to exclude the cusp region (the cusp region is usually located at distance with $|Z\ (\mathrm{GSM})| > 8\ R_E$). Since the local B_x (GSM) will change sign when crossing the current sheet, we select $B_x > 0$ (< 0) for the nightside Northern Hemisphere (Southern Hemisphere). Data with $B_x < 0$ (> 0) could be selected for the dayside Northern Hemisphere (Southern Hemisphere). Since our study is focused on the energetic ion distribution in a general condition, measurements with *SYM-H* > -50 nT were selected to minimize the influence of the extreme events during the geomagnetic storms. In this study, the IMF B_y and B_z as well as the spatial distributions of the ions are given in GSM coordinates. Therefore, the dependence on the dipole tilt/season has already partially been taken into account. Radial distances are also chosen to be greater than $R > 6\ R_E$ to avoid possible contaminations in the radiation belts [*Kronberg et al.*, 2016].

To investigate the dependence of the energetic ion distributions in the dayside magnetosphere and near-Earth plasma sheet on the IMF directions, we divide the IMF directions into four categories. They are (i) $B_z > 0$, $B_y < 0$; (ii) $B_z > 0$, $B_y > 0$; (iii) $B_z < 0$, $B_y < 0$; and (iv) $B_z < 0$, $B_y > 0$. Figure 1 shows the location of

Table 1. Median Solar Wind Parameters for Making the Magnetopause Shear Angle Plot (Figure 1)[a]

IMF Direction	B_x (nT)	B_y (nT)	B_z (nT)	Density ($1/cm^3$)	Velocity (km/s)
$B_z < 0 B_y > 0$	−1.63	2.52	−1.56	4.44	418.8
$B_z < 0 B_y < 0$	1.68	−2.48	−1.44	4.31	417.9
$B_z > 0 B_y > 0$	−1.27	2.44	1.74	4.43	416.8
$B_z > 0 B_y < 0$	1.64	−2.54	1.85	4.32	415.5

[a]The values correspond to the solar wind parameters under which the energetic ion distributions (Figures 2–5) are made.

the magnetic reconnection at the region of the magnetopause. The location is indicated by the magnetic shear angle under specific solar wind parameters (IMF direction, solar wind density, and speed), which corresponds to the median solar wind conditions during the ion observations. The magnetopause shear angle is determined from the geomagnetic field and the IMF field direction at the magnetopause. The geomagnetic field is calculated from the T96 model, and the solar wind parameters are determined by the corresponding median values (list in Table 1) of our observations in Figures 2–5 for each IMF B_y and B_z direction. The thin white line represents the line of maximum magnetic shear angles that are thought to be the most likely locations for reconnection to occur [*Trattner et al.*, 2007]. Since July was the most common month when our measurements were made, in simulations for determining the shear angle July was used for calculations of the average tilt angle (not shown here). More details about the magnetopause shear angle calculation can be found in *Trattner et al.* [2004, 2007, 2010, 2011]. Figure 1 shows the shear angle under southward (top row) and northward (bottom row) IMFs. The black ellipse in each panel represents the location of the $x = 0$ plane, which separates the dayside magnetopause (inside the circle) from the nightside magnetopause (outside the circle) of the Earth. It is worth noting that the location of reconnection is at low latitudes for southward IMF and at high latitudes for northward IMF. We also point out that energetic particles from the quasi-parallel bow shock may enter the magnetosphere through the reconnection.

3. Results

Table 2 shows the asymmetry index of the H^+ and O^+ under different IMF directions for four different Z (GSM) ranges: $4\ R_E < Z < 8\ R_E$, $0\ R_E < Z < 8\ R_E$, $-4\ R_E < Z < 0\ R_E$, $-8\ R_E < Z < -4\ R_E$. The asymmetry index is calculated using the following formula: Index $= \frac{F_{\text{dusk}} - F_{\text{dawn}}}{F_{\text{dusk}} + F_{\text{dawn}}} \times 100\%$, where F_{dusk} and F_{dawn} are median intensities at the duskside (Y (GSM) > 0, in regions I, II, and III in Figures 2–5) and dawnside (Y (GSM) < 0, in regions IV, V, and VI), respectively. The asymmetry index measures the degree of dawn-dusk asymmetry of the energetic ion intensities. Positive asymmetry index means that the ion intensities in the duskside are stronger than those in the dawnside, whereas negative asymmetry index values indicate dawnward asymmetry.

As can be seen in Table 2, the index appears to be positive for all the Z (GSM) ranges under four IMF directions for both H^+ and O^+. This indicates that the energetic ion intensities in the duskside are always stronger than those in the dawnside. This shows that the curvature-gradient drift plays important role in controlling the energetic ion dawn-dusk asymmetry. The drift dominates other effects that can lead to dawn-dusk asymmetry. This is, for example, the asymmetric reconnection under different IMF directions. The asymmetry index is larger when reconnection is located at the duskside than at the dawnside for the same Z (GSM) ranges. This strongly indicates that the reconnection location does influence the energetic ion distributions. The extent of the dusk asymmetry changes with Z (GSM) distance. For example, at $B_z < 0$ and $0 < Z < 4\ R_E$, we consider the H^+ in the Northern Hemisphere. The asymmetry index is 52.12% under $B_y > 0$ (reconnection is located at the duskside) compared to 20.40% under $B_y < 0$ (reconnection is located at the dawnside). This indicates that under $B_y < 0$ the duskward asymmetry becomes weaker. If we consider that the curvature-gradient drift has the same effect under different B_y directions at this Z range, then the reconnection location can cause about 31.72% difference of the ion distribution asymmetry. However, the difference is 7.38% when we consider region at $4 < Z < 8\ R_E$. This is consistent with the location of reconnection at lower latitudes under southward IMF (see Figure 1), which leads to stronger asymmetries there.

During northward IMF ($B_z > 0$), we also consider H^+ in the Northern Hemisphere. The asymmetry index shows clear dependence on reconnection location. The asymmetry with respect to the Z distance is, however, different from that under southward IMFs. The asymmetry index is 38.73% under $B_y > 0$ and 29.97% under

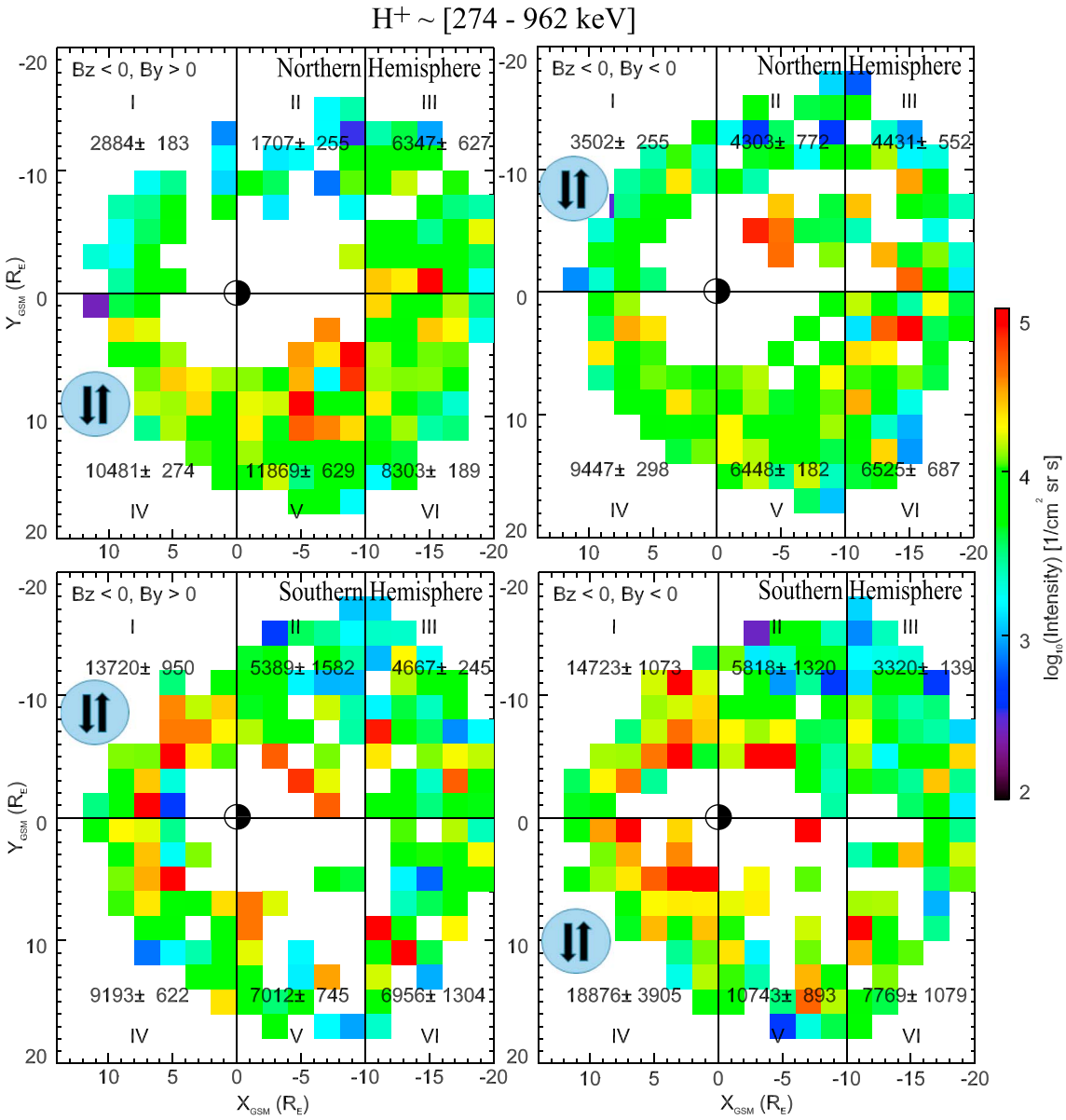

Figure 2. Proton intensities with energy from ~274 keV to ~962 keV under southward IMF with different B_y directions in both the Northern and Southern Hemispheres. The value for each bin is calculated by using the median value of the intensities of the 2 $R_E \times 2$ R_E square region when there are more than 10 measurements. Each panel is divided into six plasma sheet regions. They are (I) dayside dawn, (II) nightside near-Earth dawn, (III) tail dawn, (IV) dayside dusk flanks, (V) nightside near-Earth dusk, and (VI) tail dusk. Median values of the intensities along with the 95% confidence interval for each region are plotted in each panel. The gray circles with antiparallel arrows indicate quadrants where the magnetic shear angle becomes close to 180°.

$B_y < 0$ at $0 < Z < 4$ R_E. The asymmetry difference is 8.76%. This difference becomes larger (32.39%) when Z distance changes to $4 < Z < 8$ R_E. This is also consistent with the location of reconnection at higher latitudes under northward IMF, which leads to stronger asymmetries there (see Figure 1).

The asymmetry indexes in 0 $R_E < Z < 4$ R_E under southward IMFs and 4 $R_E < Z < 8$ R_E under northward IMFs are also plotted above Figure 1, in which the asymmetry indexes are influenced remarkably by the reconnection locations.

Similar features can be also found in the Southern Hemisphere and also for the oxygen ions. In the text below, we study the results by separating the observations into three regions: dayside magnetosphere, near-Earth nightside, and tail plasma sheet. This can give more detailed information about the energetic hydrogen and oxygen ion distributions.

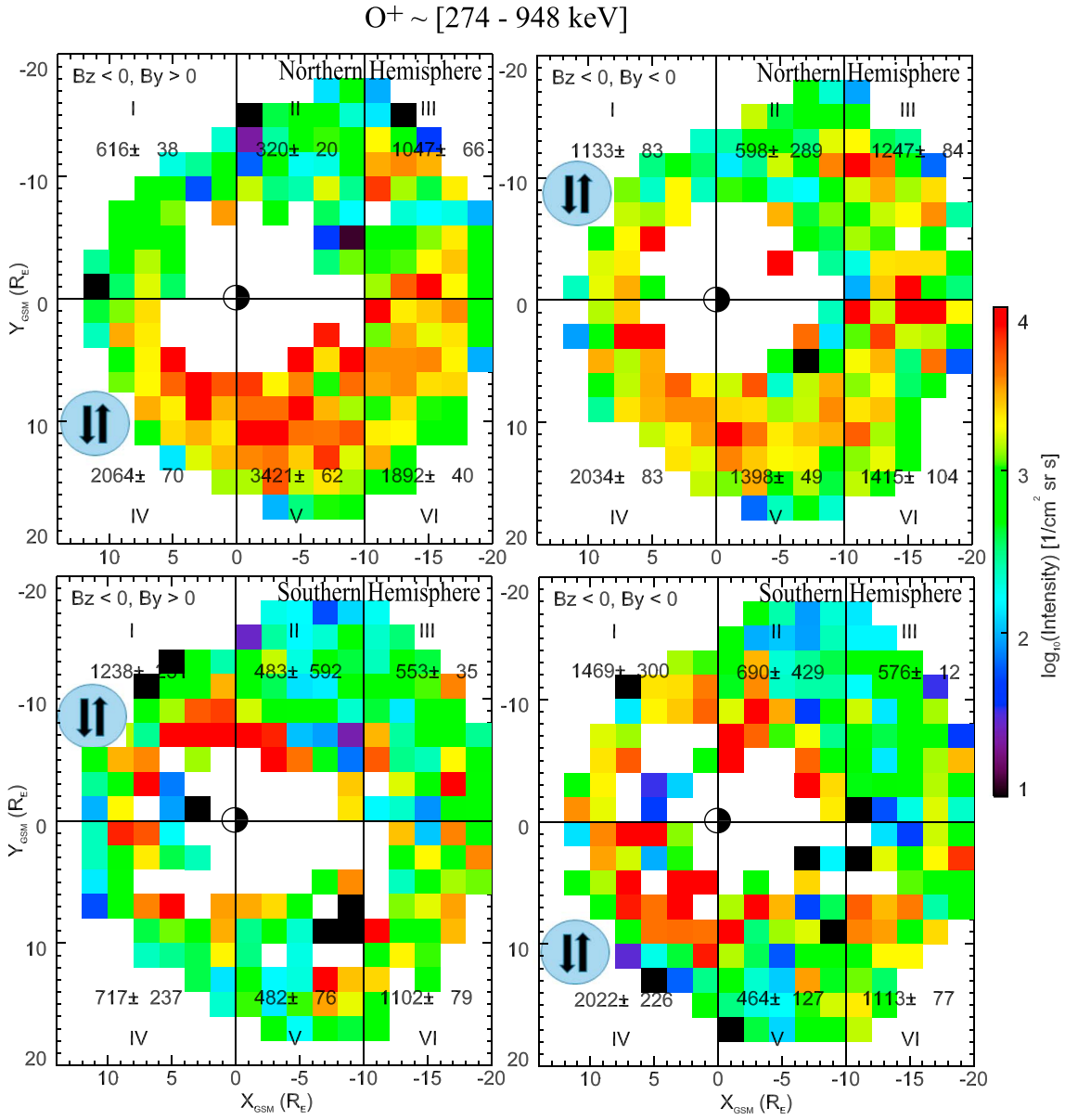

Figure 3. The format is identical to that of Figure 2 but for the oxygen ions with energy from ~274 keV to ~948 keV under southward IMF.

Figures 2–5 show the integrated intensity of energetic protons with energy from ~274 keV to ~962 keV and oxygen ions from ~274 keV to ~948 keV under different IMF B_y and B_z directions for both hemispheres. Median values of the intensities are plotted in each region. Confidence interval (CI) errors are also overplotted in each region to indicate whether the values are significantly confident based on the following formula: $\bar{x} - \frac{c_1 s}{\sqrt{n}} < \mu < \bar{x} + \frac{c_2 s}{\sqrt{n}}$, where $\bar{x}$, s, and n are the mean value, standard deviation, and sampling number in each region, respectively. Since data in each region follow a quasi-normal distribution (not shown here), the parameters c_1 and c_2 in the above formula can be determined by calculating a 95% confidence interval for each region.

3.1. Southward IMF

During southward IMF with positive B_y (Figure 2, top left), we can see a clear dawn-dusk asymmetry in the Northern Hemisphere. The intensity of H^+ is remarkably higher at the duskside than that at the dawnside

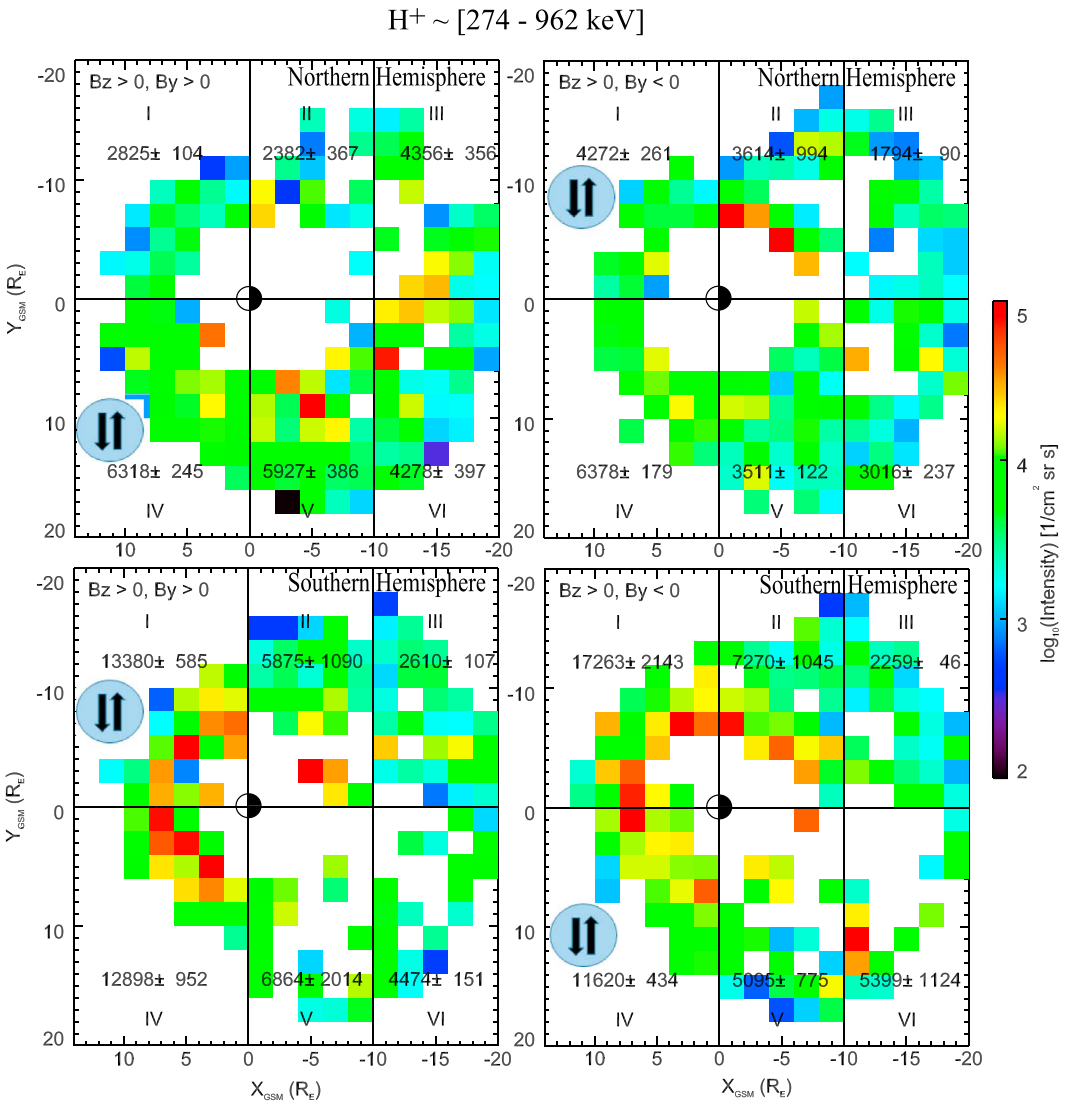

Figure 4. The format is identical to that of Figure 2 but for the protons with energy from ~274 keV to ~962 keV under northward IMFs.

for both the dayside magnetosphere and nightside plasma sheet. This is expected for distributions governed by gradient and curvature drifts. However, this duskside asymmetry is absent in the Southern Hemisphere at the dayside. On the contrary, the H^+ intensity (bottom left) at the dawnside of dayside magnetosphere (region I) is even stronger than those at the corresponding duskside regions (regions IV). This dawn-dusk asymmetry is quite consistent with the reconnection location under that IMF orientation. When the IMF $B_z < 0$ and $B_y > 0$, reconnection is located in the sunward dusk (sunward dawn) sector in the Northern (Southern) Hemisphere.

When IMF B_y is directed dawnward (Figure 2, top right), although the intensity at the duskside is still stronger than that at the dawnside for the Northern Hemisphere, the asymmetry is not that prominent as that under positive IMF B_y at least between regions I and IV, II, and V (top left). We believe that the duskward asymmetry due to the curvature and magnetic gradient drift is weakened by an additional dawnside ion source related to the reconnection at the magnetopause during this IMF orientation. For the Southern Hemisphere with negative IMF B_y (bottom right), both the drift effect and reconnection location force ions to prefer the duskside. The stronger flux areas indeed appear at the duskside regions.

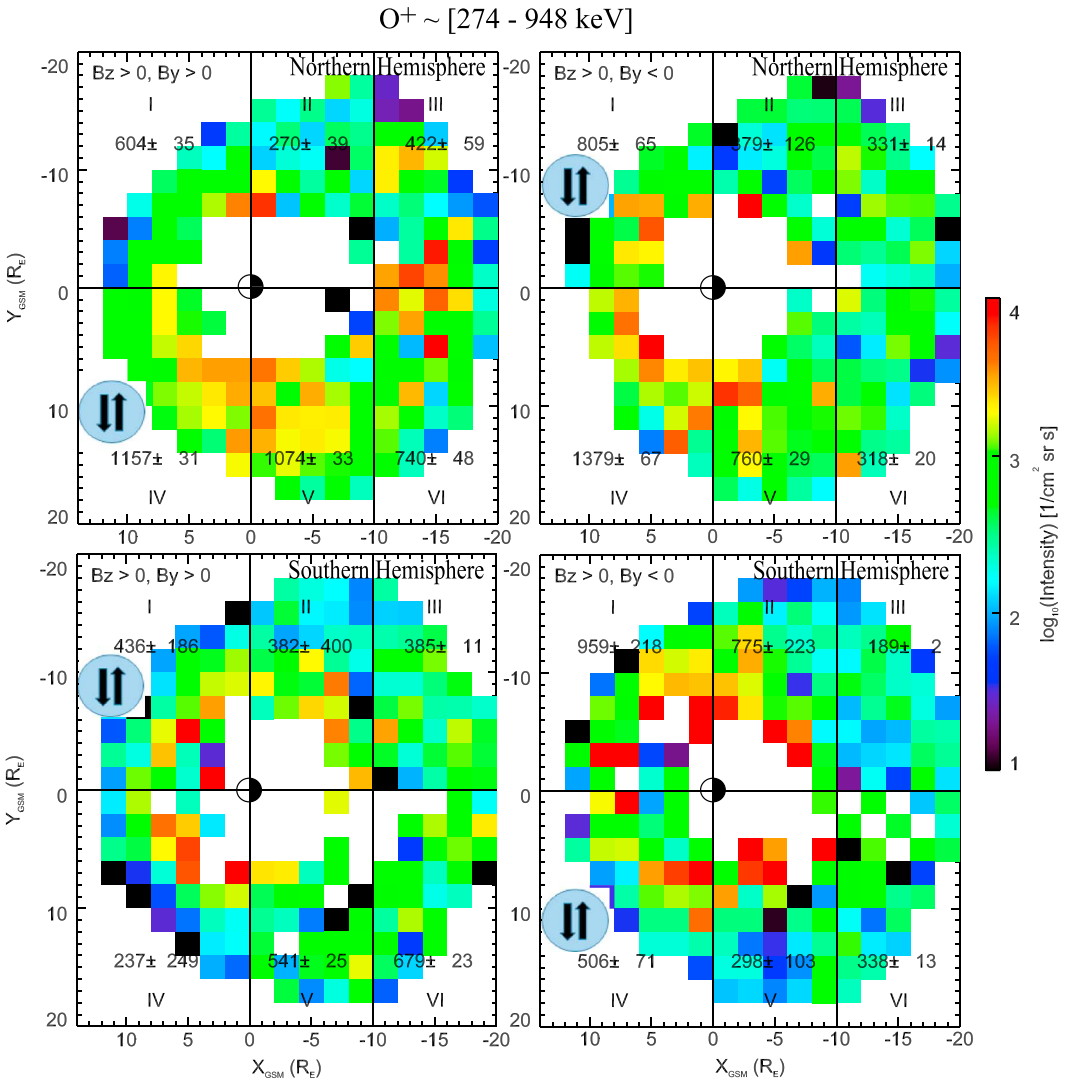

Figure 5. The format is identical to that of Figure 2 but for oxygen ions with energy from ~274 keV to ~948 keV under northward IMFs.

The intensity distributions of O^+ during southward IMF under different IMF B_y directions for both Northern and Southern Hemispheres are shown in Figure 3. The layout of Figure 3 is the same as of Figure 2. The asymmetries in the Northern Hemisphere for oxygen ions are nearly the same as for protons under both positive and negative IMF B_y. This indicates that the IMF B_y exerts the same effect on dawn-dusk asymmetries for oxygen ions and protons.

For the Southern Hemisphere and positive IMF B_y (bottom left), the intensity at dawnside of the dayside region I is stronger than the corresponding flux at the duskside region IV and basically the same between regions II and V at the near-Earth nightside. This is also in very good agreement with reconnection at the dawn sector under southward IMF with positive IMF B_y. The dawnside asymmetry is not seen at the tail region (III and VI in Figure 3, bottom left) where the flux at the duskside is stronger than at the dawnside which indicates that the drift processes are more important in the tail region.

During negative IMF B_y, the oxygen ion intensity at the duskside of the dayside magnetosphere in the Southern Hemisphere becomes stronger compared to those for positive IMF B_y. This agrees with the fact that in the Southern Hemisphere, for negative IMF B_y, reconnection occurs at the duskside. This could lead to the escape of energetic ions to the duskside and therefore lead to a weakening of the dawnward asymmetry. The large confidence intervals do not allow us to give a definite conclusion for the

Table 2. Asymmetry Index of the H^+ and O^+ Under Different IMF Directions for Four Different Z (GSM) Ranges[a]

		IMF Direction			
		$B_z < 0$ $B_y > 0$	$B_z < 0$ $B_y < 0$	$B_z > 0$ $B_y > 0$	$B_z > 0$ $B_y < 0$
Northern Hemisphere					
Reconnection Location		Duskside	Dawnside	Duskside	Dawnside
H^+	$4\ R_E < Z < 8\ R_E$	34.49%	27.87%	51.60%	19.21%
	$0\ R_E < Z < 4\ R_E$	52.12%	20.40%	38.73%	29.97%
O^+	$4\ R_E < Z < 8\ R_E$	47.81%	30.14%	44.74%	13.43%
	$0\ R_E < Z < 4\ R_E$	61.60%	28.71%	39.42%	28.93%
Southern Hemisphere					
Reconnection Location		Dawnside	Duskside	Dawnside	Duskside
H^+	$-8\ R_E < Z < -4\ R_E$	12.14%	19.89%	9.15%	21.44%
	$-4\ R_E < Z < 0\ R_E$	21.26%	49.13%	18.99%	30.81%
O^+	$-8\ R_E < Z < -4\ R_E$	11.45%	31.43%	10.67%	22.94%
	$-4\ R_E < Z < 0\ R_E$	27.55%	36.63%	23.81%	28.65%

[a]The asymmetry index is calculated using the following formula Index $= \frac{F_{\text{dusk}} - F_{\text{dawn}}}{F_{\text{dusk}} + F_{\text{dawn}}} \times 100\%$, where F_{dusk} and F_{dawn} are median intensities at the duskside (Y (GSM) > 0, in regions I, II, and III in Figures 2–5) and dawnside (Y (GSM) < 0, in regions IV, V, and VI), respectively. Reconnection location is indicated for each direction of the IMF and for two hemispheres.

near-Earth nightside (regions II and V). In the tail region (regions III and VI) the duskward asymmetry is observed.

3.2. Northward IMF

During northward IMF, the dawn-dusk asymmetries are expected to be the same as during southward IMF (see Figure 1). However, the location of reconnection will be at higher latitudes during northward IMF. As can be seen in Figures 4 and 5, in general, the H^+ and O^+ intensities are significantly lower during northward IMF than that during southward IMF especially at the dusk for both dayside magnetosphere and nightside plasma sheet. During southward IMF, the energy coupling between solar wind and magnetosphere is much stronger than that during northward IMF. Therefore, the inductive electric field [e.g., *Delcourt*, 2002] or dipolarization fronts related magnetic reconfiguration [*Nosé et al.*, 2000b] are stronger during southward IMFs, which can result in more energetic ions (>100 keV) in the magnetotail. The large-scale dawn-dusk electric field drift along with the gradient-curvature drift makes the energetic ions move to the dusk flanks.

We can see in Figure 4 that in the Northern Hemisphere a clear dusk asymmetry appears with positive IMF B_y, which is in good agreement with both duskward drift and location of reconnection at the duskside. This asymmetry, however, becomes weaker when IMF B_y directs dawnward, especially between the near-Earth nightside regions II and V, where the intensities are nearly the same. The weaker duskward asymmetry is because although the curvature and gradient drift still force high-energy ions to move to the duskside plasma sheet, reconnection can provide a source in the dawn near-Earth sector tailward of the cusp in the Northern Hemisphere which leads to the weakening duskside asymmetry. These features are similar to those with the southward IMFs in the Northern Hemisphere. As long as the IMF B_y is pointing to the dawnside or duskside, reconnection occurs in the same direction as the IMF B_y in the Northern Hemisphere, which is independent on the IMF B_z.

The dawn-dusk location of reconnection in the Southern Hemisphere has the opposite direction of IMF B_y and also independent on the IMF B_z. Rotation of the IMF from southward to northward moves location of reconnection from sunward side of the cusp to the tailward side. Under positive IMF B_y, the asymmetry in the Southern Hemisphere at the dayside appears to be dawnward for both H^+ and O^+ ions; see bottom left panels in Figures 4 and 5. This is also consistent with the location of reconnection at the dawnside.

Under negative IMF B_y the intensities at the dayside and near-Earth nightside dawn are significantly higher than corresponding intensities at the duskside for hydrogen and oxygen ions (bottom right panels of Figures 4 and 5). We observe higher ion intensities at the dawnside, although they are expected to be higher at the duskside according to the location of reconnection. This inconsistency can be explained as follows. From the map of samples (see supporting information) one can see that the spacecraft spent much less time at the duskside in the Southern Hemisphere than at the dawnside, especially at high latitudes. Under the northward IMF an ion source related to location of reconnection is expected to be at high latitudes; see Figure 1. Therefore, these regions were likely not measured. This can explain lower intensities at the dusk dayside compare to those at the dawnside in the Southern Hemisphere. The statistical coverage becomes less significant when we do not divide the data into the three regions, and the statistics is enough to get

Table 3. Median Values of the Energetic Ion (H^+ From 274 keV to 962 keV and O^+ From 274 keV to 948 keV) Intensities [1/(cm^2 sr s)] Correspond to the Different Regions in Figures 2–5 Under Four Different IMF Directions[a]

IMF Direction	Ion Species	Region I	Region II	Region III	Region IV	Region V	Region VI
$B_z < 0 B_y > 0$	Northern Hemisphere						
	H^+	2,884 ± 183	1,707 ± 255	6,347 ± 627	10,481 ± 274	11,869 ± 629	8,303 ± 189
	O^+	616 ± 38	320 ± 20	1,047 ± 66	2,064 ± 70	3,421 ± 62	1,892 ± 40
	Southern Hemisphere						
	H^+	13,720 ± 950	5,389 ± 1,582	4,667 ± 245	9,193 ± 622	7,102 ± 745	6,956 ± 1,304
	O^+	1,238 ± 251	483 ± 592	553 ± 35	717 ± 237	482 ± 76	1,102 ± 79
$B_z < 0 B_y < 0$	Northern Hemisphere						
	H^+	3,502 ± 255	4,302 ± 772	4,431 ± 552	9,447 ± 298	6,448 ± 182	6,525 ± 687
	O^+	1,133 ± 83	598 ± 289	1,247 ± 84	2,034 ± 83	1,398 ± 49	1,415 ± 104
	Southern Hemisphere						
	H^+	14,723 ± 1,073	5,818 ± 1,320	3,320 ± 139	18,876 ± 3,905	10,743 ± 893	7,769 ± 1,079
	O^+	2,022 ± 226	690 ± 429	576 ± 12	1,469 ± 300	464 ± 127	1,113 ± 77
$B_z > 0 B_y > 0$	Northern Hemisphere						
	H^+	2,825 ± 104	2,382 ± 367	4,356 ± 356	6,318 ± 245	5,927 ± 386	4,278 ± 397
	O^+	604 ± 35	270 ± 39	422 ± 59	1,157 ± 31	1,074 ± 33	740 ± 48
	Southern Hemisphere						
	H^+	13,380 ± 585	5,875 ± 1,090	2,610 ± 107	12,898 ± 952	6,864 ± 2,014	4,474 ± 151
	O^+	436 ± 186	382 ± 400	385 ± 11	237 ± 249	541 ± 25	679 ± 23
$B_z > 0 B_y < 0$	Northern Hemisphere						
	H^+	4,272 ± 261	3,614 ± 994	1,794 ± 90	6,378 ± 179	3,511 ± 122	3,016 ± 237
	O^+	805 ± 65	379 ± 126	331 ± 14	1,379 ± 67	760 ± 29	318 ± 20
	Southern Hemisphere						
	H^+	17,263 ± 2,143	7,270 ± 1,045	2,259 ± 46	11,620 ± 434	5,095 ± 775	5,399 ± 1,124
	O^+	959 ± 218	775 ± 223	189 ± 2	506 ± 71	298 ± 103	338 ± 13

[a]These values are also plotted above each region in Figures 2–5.

confident results that show clear consistence between the observations and location of reconnection, as seen in Table 2.

In summary, we investigated the energetic ions (~274 keV to ~955 keV) distributions in the dayside magnetosphere and near-Earth plasma sheet under different IMF directions. Table 3 lists the median values of the ion intensities along with the 95% confidence intervals in different areas under four IMF directions for both the Northern and Southern Hemispheres.

4. Discussion and Conclusions

In this study, based on 11 years of ion flux of both protons (~274 keV to ~962 keV) and oxygen ions (~274 keV to ~948 keV) from Cluster/RAPID, we statistically study the dawn-dusk IMF dependence of the energetic ion distributions in the dayside magnetosphere and the plasma sheet. In fact, we also check the integrated flux from CIS instruments with H^+ and O^+ energy range from ~10 keV to ~35 keV (not shown here), which gives mainly similar IMF dependence of the dawn-dusk asymmetry. Other factors such as geomagnetic activities, solar emissions, and solar wind conditions can influence dawn-dusk asymmetries of the energetic ion distributions. Unfortunately, we cannot consider all these conditions simultaneously as there is not sufficient data to make confident maps for the distributions at these energies.

It is found in this study that the dawn-dusk asymmetry of the energetic ion distribution shows strong dependence on the IMF direction, and we attribute this dependence to the location magnetic reconnection at the magnetopause. Large-scale quasi-stationary dawn-dusk electric field or betatron acceleration alone was proved to be not enough to accelerate the ions above 100 keV. Inductive electric field associated with the fast magnetic X line formation [*Zelenyi et al.*, 1990], electromagnetic turbulence [*Grigorenko et al.*, 2015], or current disruption processes [*Lui*, 1996; *Lutsenko et al.*, 2008] are likely acceleration sources for the >100 keV energetic ions. However, such mechanisms usually occurred in the magnetotail, and they alone cannot explain the dawn-dusk asymmetries of the energetic oxygen and hydrogen ion distributions. One may argue that the *E* cross *B* drift could result in the asymmetry. However, the *E* cross *B* along with the gradient and curvature drift can only explain the duskside asymmetry of energetic ions at these energies. The

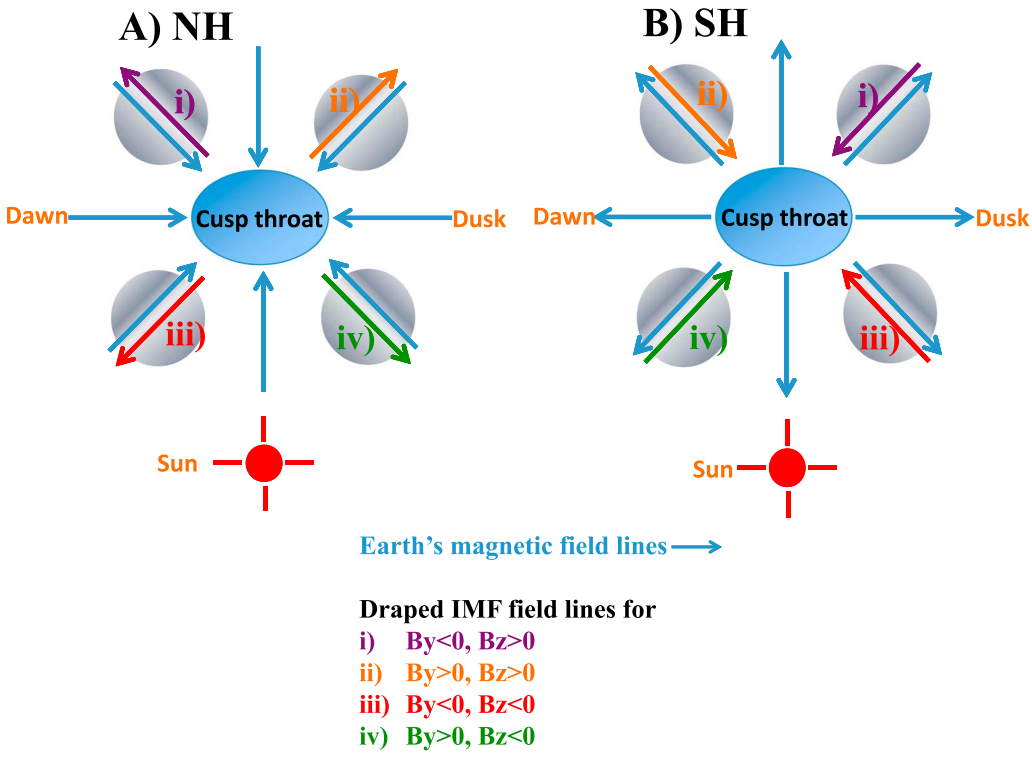

Figure 6. The Earth's magnetic field and the draped IMFs for each orientation. Shaded gray regions indicate under each IMF orientation where the most antiparallel components are located relative to the cusp region and also the diamagnetic cavity can form and trap the particles. The location of the Sun is indicated by the red circles.

drift cannot explain dawnside asymmetry observed in the Southern Hemisphere under duskward southward IMF and weakening of the asymmetry in the Northern Hemisphere under dawnward northward IMF. Therefore, some local acceleration and/or transport processes other than drifts should occur at near-Earth nightside and/or dayside region.

Magnetic reconnection could occur at low-latitude magnetopause (during southward IMF, for example) where the IMF and the magnetic field from the magnetosphere have opposite directions. Some energetic particles with large gyroradius from the quasi-parallel bow shock can enter the magnetosphere via reconnection at the magnetopause. Energetic ions can penetrate the magnetosphere across the magnetopause current sheet via, e.g., Speiser motion. This well agrees with the observations under the southward IMF. The asymmetry index is stronger at low latitudes than at high latitudes. This indicates that ions enter the magnetosphere at low latitudes and not from, for example, a diamagnetic cavity located at high latitudes; see Figure 6.

During reconnection at the magnetopause ions do not necessarily directly penetrate the magnetosphere. Solar wind ions can be also accelerated at the reconnection region (not necessary up to hundreds of keV) and be transported toward the cusp. Energetic particles from the quasi-parallel bow shock can also enter the diamagnetic cavity and populate it [*Trattner et al.*, 2011]. The quasi-parallel bow shock can be a source of energetic ions in the cusp [e.g., *Trattner et al.*, 2001, 2010, *Lin et al.*, 2007]. However, it is quite hard to explain the frequently observed high-energy electrons and singly charged oxygen ions in the cusp region, if the bow shock is the only source [*Nykyri et al.*, 2012].

The particles transported toward the cusp get accumulated there and lead to the enhanced plasma pressure, which is compensated by the drop in the magnetic field. Reconnection will also occur in the cusp region if IMF and the local magnetic field in the cusp region have opposite directions along with the enhanced plasma pressure and therefore lead to formation of the diamagnetic cavity; see Figure 6. Particles in the diamagnetic cavity will experience efficient local acceleration if they are trapped for sufficiently long time in the cavity and their drift paths coincide with the gradient of reconnection quasi-potential because reconnection alone

without cavity formation cannot energize such a vast flux of the energetic ions [*Nykyri et al*., 2011a, 2011b, 2012]. The location of the diamagnetic cavities depends on the IMF directions [*Nykyri et al*., 2011a]; see Figure 6. The energetic particles in the diamagnetic cavity can leak directly into the magnetosheath; see, for example, the simulations in *Nykyri et al.* [2012]. The energetic ions in the magnetosheath at high latitudes can be then transported in the magnetosphere via, for example, the Kelvin-Helmholtz instability (see, e.g., review in *Wing et al.* [2014] also about other entry processes, *Kavosi and Raeder* [2015], and observations of Kelvin-Helmholtz instability at high-latitude magnetopause by *Hwang et al.* [2012]).

The transportation processes due to Kelvin-Helmholtz instability is in the order of 10s of seconds (e.g., *Smets et al.* [2002] have estimated that at least one ion from 10 to 50 gyroperiods crosses the magnetopause and enter the magnetosphere during developing Kelvin-Helmholtz instabilities). Even without a Kelvin-Helmholtz instability, energetic ions with gyroradii larger than size of a diamagnetic cavity can cross the magnetopause current sheet and enter the magnetosphere during, e.g., Speiser motion trajectories.

Under northward IMF our statistics for high latitudes at $4\ R_E < |Z| < 8\ R_E$ shows higher asymmetry index for quadrants where the location of a diamagnetic cavity is predicted (see Table 2 and Figure 6). The scenario of energetic ion transport from the diamagnetic cavity to the magnetosphere is also consistent with our observations showing that the ion fluxes are significantly more intense in the inner regions where diamagnetic cavities are more likely to be located than in the outer regions for a northward IMF (Figures 4 and 5). The enhancement of the particle flux due to the adiabatic transport would show a more gradual pattern in radially outward direction. As location of the diamagnetic cavity is dependent on the IMF direction, this can lead to the observed asymmetry in the energetic ion population in the dayside magnetosphere and plasma sheet. However, this does not exclude a direct penetration via reconnection of energetic ions from the quasi-parallel bow shock as asymmetry is the same.

From the analysis above, we can conclude the following:

1. The energetic ion distributions in the near-Earth plasma sheet are strongly dependent on the IMF direction in both Northern and Southern Hemispheres: the duskside/dawnside asymmetry of the energetic ion distributions appears with the positive IMF B_y in the Northern/Southern Hemisphere for both southward and northward IMF. Negative IMF B_y can weaken/strengthen the duskside/dawnside asymmetries in Northern/Southern Hemisphere.
2. We propose that the observed dawn-dusk asymmetry can be explained by gradient/curvature drift of energetic ions in combination with a source governed by magnetic reconnection at the magnetopause.
3. The distributions of energetic oxygen ions have the same dawn-dusk asymmetry as the protons with respect to the IMF direction. This indicates that they experience the same transport processes.

The identification of most effective mechanisms at populating the magnetosphere with energetic particles is the task for further studies.

Acknowledgments

We acknowledge the Deutsches Zentrum für Luft und Raumfahrt (DLR) for supporting the RAPID instrument at MPS under grant 50 OC 1602. We thank useful discussions during team meetings on "Heavy ions: their dynamical impact on the magnetosphere" at the International Space Science Institute (ISSI). The work by K. Nykyri was supported by NASA grant 15-HGI15_2-0187. The solar wind data are provided by the OMNI database from CDAWeb. This work was supported by the Key Program of the National Natural Science Foundation of China (41590851). The Cluster data can be found at Cluster Science Archive (CSA): http://www.cosmos.esa.int/web/csa/.

References

Adamson, E., A. Otto, and K. Nykyri (2012), 3-D mesoscale MHD simulations of magnetospheric cusp-like configurations: Cusp diamagnetic cavities and boundary structure, *Ann. Geophys.*, *30*, 325–341, doi:10.5194/angeo-30-325-2012.

Balogh, A., et al. (2001), The Cluster magnetic field investigation: Overview of in-flight performance and initial results, *Ann. Geophys.*, *19*, 1207–1217.

Chen, J. S., and T. A. Fritz (1998), Correlation of cusp MeV helium with turbulent ULF power spectra and its implications, *Geophys. Res. Lett.*, *25*, 4113–4116.

Baumjohann, W., G. Paschmann, and H. Luehr (1990), Characteristics of high-speed ion flows in the plasma sheet, *J. Geophys. Res.*, *95*, 3801–3809, doi:10.1029/JA095iA04p03801.

Dandouras, I., A. Barthe, E. Penou, H. Rème, S. McCaffrey, C. Vallat, L. M. Kistler, and The Cis Team (2006), Cluster Ion Spectrometry (CIS) data in the Cluster Active Archive (CAA), Eur. Space Agency Spec. Publ., ESA SP-598.

Delcourt, D. C. (2002), Particle acceleration by inductive electric fields in the inner magnetosphere, *J. Atmos. Sol. Terr. Phys.*, *64*, 551–559, doi:10.1016/S1364-6826(02)00012-3.

Escoubet, C. P., R. Schmidt, and M. L. Goldstein (1997), Cluster—Science and mission overview, *Space Sci. Rev.*, *79*, 11–32.

Fritz, T. A., A. Theodore, J. Chen, and R. B. Sheldon (2000), The role of the cusp as a source for magnetospheric particles: A new paradigm?, *Adv. Space Res.*, *25*(7–8), 1445–1457.

Fritz, T. A., B. M. Walsh, M. Klida, and J. Chen (2012), The cusp as a source of magnetospheric particles, *J. Atmos. Sol. Terr. Phys.*, *87*, 39–46, doi:10.1016/j.jastp.2011.10.016.

Grigorenko, E. E., R. Kolvea, and J.-A. Sauvaud (2012), On the problem of plasma sheet boundary layer identification from plasma moments in Earth's magnetotail, *Ann. Geophys.*, *30*(9), 1331–1343, doi:10.5194/angeo-30-1331-2012.

Grigorenko, E. E., A. Y. Malykhin, E. A. Kronberg, K. V. Malova, and P. W. Daly (2015), Acceleration of ions to suprathermal energies by turbulence in the plasmoid-like magnetic structures, *J. Geophys. Res. Space Physics*, *120*, 6541–6558, doi:10.1002/2015JA021314.

Grigorenko, E. E., E. A. Kronberg, and P. W. Daly (2017), Heating and acceleration of charged particles during magnetic field dipolarizations, *Cosmic Res.*, *55*(1), 57–66, doi:10.1134/S0010952517010063.

Hwang, K.-J., M. L. Goldstein, M. M. Kuznetsova, Y. Wang, A. F. Vinas, and D. G. Sibeck (2012), The first in situ observation of Kelvin-Helmholtz waves at high-latitude magnetopause during strongly dawnward interplanetary magnetic conditions, *J. Geophys. Res.*, *117*, A08233, doi:10.1029/2011JA017256.

Kavosi, S., and J. Raeder (2015), Ubiquity of Kelvin-Helmholtz waves at Earth's magnetopause, *Nat. Commun.*, *6*, 7019, doi:10.1038/ncomms8019.

Kronberg, E. A., S. E. Haaland, P. W. Daly, E. E. Grigorenko, L. M. Kistler, M. Fränz, and I. Dandouras (2012), Oxygen and hydrogen ion abundance in the near-Earth magnetosphere: Statistical results on the response to the geomagnetic and solar wind activity conditions, *J. Geophys. Res.*, *117*, A12208, doi:10.1029/2012JA018071.

Kronberg, E. A., E. E. Grigorenko, S. E. Haaland, P. W. Daly, D. C. Delcourt, H. Luo, L. M. Kistler, and I. Dandouras (2015), Distribution of energetic oxygen and hydrogen in the near-Earth plasma sheet, *J. Geophys. Res. Space Physics*, *120*, 3415–3431, doi:10.1002/2014JA020882.

Kronberg, E. A., et al. (2016), Contamination in electron observations of the silicon detector onboard Cluster/RAPID/IES instrument in Earth's radiation belts and ring current, *Space Weather*, *14*, 449–462, doi:10.1002/2016SW001369.

Kronberg E. A., K. Li, E.E. Grigorenko, R. Maggiolo, S. E. Haaland, P. W. Daly and H. Luo (2017), Dawn-dusk asymmetries in the near-Earth plasma sheet: Ion observations, in Book "*Dawn-Dusk Asymmetries in Planetary Plasma Environments*," *Geophys. Monogr. Ser.*, 228, Washington D. C.

Liao, J., L. M. Kistler, C. G. Mouikis, B. Klecker, I. Dandouras, and J.-C. Zhang (2010), Statistical study of O^+ transport from the cusp to the lobes with Cluster CODIF data, *J. Geophys. Res.*, *115*, A00J15, doi:10.1029/2010JA015613.

Lin, Y., X. Y. Wang, and S.-W. Chang (2007), Connection between bow shock and cusp energetic ions, *Geophys. Res. Lett.*, *34*, L11107, doi:10.1029/2007GL030038.

Lui, A. T. Y. (1996), Current disruption in the Earth's magnetosphere: Observations and models, *J. Geophys. Res.*, *101*, 13,067–13,088, doi:10.1029/96JA00079.

Luo, H., E. A. Kronberg, E. E. Grigorenko, M. Fraenz, P. W. Daly, G. X. Chen, A. M. Du, L. M. Kistler, and Y. Wei (2014), Evidence of strong energetic ion acceleration in the near-Earth magnetotail, *Geophys. Res. Lett.*, *41*, 3724–3730, doi:10.1002/2014GL060252.

Lutsenko, V. N., E. A. Gavrilova, and T. V. Grechko (2008), Statistics of fine dispersion structures events in energetic particle spectra: Their origin and role in the outer magnetosphere, *Ann. Geophys.*, *26*, 2097–2110, doi:10.5194/angeo-26-2097-2008.

Nosé, M., A. T. Y. Lui, S. Ohtani, B. H. Mauk, R. W. McEntire, D. J. Williams, T. Mukai, and K. Yumoto (2000a), Acceleration of oxygen ions of ionospheric origin in the near-Earth magnetotail during substorms, *J. Geophys. Res.*, *105*(A4), 7669–7677, doi:10.1029/1999JA000318.

Nosé, M., S. Ohtani, A. T. Y. Lui, S. P. Christon, R. W. McEntire, D. J. Williams, T. Mukai, Y. Saito, and K. Yumoto (2000b), Change of energetic ion composition in the plasma sheet during substorms, *J. Geophys. Res.*, *105*(A10), 23277–23286, doi:10.1029/2000JA000129.

Nykyri, K., A. Otto, E. Adamson, E. Dougal, and J. Mumme (2011a), Cluster observations of a cusp diamagnetic cavity: Structure, size and dynamics, *J. Geophys. Res.*, *116*, A03228, doi:10.1029/2010JA015897.

Nykyri, K., A. Otto, E. Adamson, and A. Tjulin (2011b), On the origin of fluctuations in the cusp diamagnetic cavity, *J. Geophys. Res.*, *116*, A06208, doi:10.1029/2010JA015888.

Nykyri, K., A. Otto, E. Adamson, E. Kronberg, and P. Daly (2012), On the origin of high-energy particles in the cusp diamagnetic cavity, *J. Atmos. Sol. Terr. Phys.*, *87*(2012), 70–81, doi:10.1016/j.jastp.2011.08.012.

Ono, Y., M. Nosé, S. P. Christon, and A. T. Y. Lui (2009), The role of magnetic field fluctuations in nonadiabatic acceleration of ions during dipolarization, *J. Geophys. Res.*, *114*, A05209, doi:10.1029/2008JA013918.

Petrinec, S. M., et al. (2011), Neutral atom imaging of the magnetospheric cusps, *J. Geophys. Res.*, *116*, A07203, doi:10.1029/2010JA016357.

Rème, H., et al. (2001), First multispacecraft ion measurements in and near the Earth's magnetosphere with the identical Cluster ion spectrometry (CIS) experiment, *Ann. Geophys.*, *19*, 1303–1354.

Smets, R., D. Delcourt, G. Chanteur, and T. E. Moore (2002), On the incidence of Kelvin-Helmholtz instability for mass exchange process at the Earth's magnetopause, *Ann. Geophys.*, *20*, 757–769.

Speiser, T. W. (1965), Particle trajectories in model current sheets: 1. Analytical solutions, *J. Geophys. Res.*, *70*, 4219–4226, doi:10.1029/JZ070i017p04219.

Sarafopoulos, D. V., N. F. Sidiropoulos, E. T. Sarris, V. Lutsenko, and K. Kudela (2001), The dawn-dusk plasma sheet asymmetry of energetic particles: An interball perspective, *J. Geophys. Res.*, *106*, 13,053–13,066, doi:10.1029/2000JA900157.

Trattner, K. J., S. A. Fuselier, W. K. Peterson, S.-W. Chang, R. Friedel, and M. R. Aellig (2001), Origins of energetic ions in the cusp, *J. Geophys. Res.*, *106*, 5967–5976.

Trattner, K. J., S. A. Fuselier, and S. M. Petrinec (2004), Location of the reconnection line for northward interplanetary magnetic field, *J. Geophys. Res.*, *109*, A03219, doi:10.1029/2003JA009975.

Trattner, K. J., J. S. Mulcock, S. M. Petrinec, and S. A. Fuselier (2007), Probing the boundary between antiparallel and component reconnection during southward interplanetary magnetic field conditions, *J. Geophys. Res.*, *112*, A08210, doi:10.1029/2007JA012270.

Trattner, K. J., S. M. Petrinec, S. A. Fuselier, W. K. Peterson, and R. Friedel (2010), Cusp energetic ions as tracers for particle transport into the magnetosphere, *J. Geophys. Res.*, *115*, A04219, doi:10.1029/2009JA014919.

Trattner, K. J., S. M. Petrinec, S. A. Fuselier, K. Nykyri, and E. Kronberg (2011), Cluster observations of bow shock energetic ion transport through the magnetosheath into the cusp, *J. Geophys. Res.*, *116*, A09207, doi:10.1029/2011JA016617.

Welling, D. T., V. K. Jordanova, S. G. Zaharia, A. Glocer, and G. Toth (2011), The effects of dynamic ionospheric outflow on the ring current, *J. Geophys. Res.*, *116*, A00J19, doi:10.1029/2010JA015642.

Wilken, B., Q.-G. Zong, I. A. Daglis, T. Doke, S. Livi, K. Maezawa, Z. Y. Pu, S. Ullaland, and T. Yamamoto (1995), Tailward flowing energetic oxygen ion bursts associated with multiple flux ropes in the distant magnetotail: Geotail observations, *Geophys. Res. Lett.*, *22*, 3267–3270.

Wilken, B., et al. (2001), First results from the RAPID imaging energetic particle spectrometer on board Cluster, *Ann. Geophys.*, *19*, 1355–1366.

Wing, S., et al. (2014), Review of solar wind entry into and transport within the plasma sheet, *Space Sci. Rev.*, *184*, 33, doi:10.1007/s11214-014-0108-9.

Zelenyi, L. M., J. G. Lominadze, and A. L. Taktakishvili (1990), Generation of the energetic proton and electron bursts in planetary magnetotails, *J. Geophys. Res.*, *95*, 3883–3891, doi:10.1029/JA095iA04p03883.

Zong, Q.-G., et al. (1997), Geotail observations of energetic ion species and magnetic field in plasmoid-like structures in the course of an isolated substorm event, *J. Geophys. Res.*, *102*(A6), 11409–11428, doi:10.1029/97JA00076.

Zong, Q.-G., et al. (1998), Energetic oxygen ion bursts in the distant magnetotail as a product of intense substorms: Three case studies, *J. Geophys. Res.*, *103*(A9), 20339–20363, doi:10.1029/97JA01146.